Numerical Heat Transfer, Part A: Applications: An International Journal of Computation and Methodology
Publication details, including instructions for authors and subscription information:
http://www.tandfonline.com/loi/unht20

SIMULTANEOUS HEAT AND MASS TRANSFER IN POLYMER SOLUTIONS EXPOSED TO INTERMITTENT INFRARED RADIATION HEATING

Jyh-Jian Chen [a] & Jenn-Der Lin [a]
[a] Department of Mechanical Engineering , National Chiao Tung University , 1001 Ta Hsueh Road, Hsinchu, Taiwan, 30050, Republic of China
Published online: 15 Mar 2007.

To cite this article: Jyh-Jian Chen & Jenn-Der Lin (1998) SIMULTANEOUS HEAT AND MASS TRANSFER IN POLYMER SOLUTIONS EXPOSED TO INTERMITTENT INFRARED RADIATION HEATING, Numerical Heat Transfer, Part A: Applications: An International Journal of Computation and Methodology, 33:8, 851-873, DOI: 10.1080/10407789808913970

To link to this article: http://dx.doi.org/10.1080/10407789808913970

SIMULTANEOUS HEAT AND MASS TRANSFER IN POLYMER SOLUTIONS EXPOSED TO INTERMITTENT INFRARED RADIATION HEATING

Jyh-Jian Chen and Jenn-Der Lin
Department of Mechanical Engineering, National Chiao Tung University, 1001 Ta Hsueh Road, Hsinchu, Taiwan 30050, Republic of China

A theoretical study is performed that describes heat transfer and moisture variation while a polymer solution is exposed to high-intensity infrared radiation flux and/or an airflow. While the intermittent heating is considered, we investigate the influences of various radiation and convection parameters on the transfer of heat and moisture variation of coated layers on an optically thick substrate. During the tempering stage in the intermittent heating process, the convective mass transfer is included to simulate the ambient air in reality. The effects of radiation and convection parameters on the transfer processes are presented in terms of the rate of water content removal, heat transfer, and moisture distributions. Numerical results show that the rate of water removal from the polymer solution is dominated by both the absorbed radiative heat energy and the distributions of water mass fraction in the polymer solution.

INTRODUCTION

Drying is one of the essential steps in a number of industrial applications, such as the preserving of food and the drying of paint, pulp, and paper. The quality of paper tubes is significantly affected by the heat and mass transfer process. The drying of polymer solution plays a crucial role in the manufacture of photographic film, synthetic fibers, adhesives, and a variety of other polymeric products. During drying of wet materials, simultaneous heat and mass transfer occurs both inside the medium and in the boundary layer of the drying agent. Drying is one of the most energy-consuming processes in the industrial sector and can also be very time consuming as, for example, in conventional convective drying by hot air, while minimum cost and energy consumption and maximum product quality are among the main concerns in industry today. Drying of water-based materials, however, is often a problem when using conventional drying methods and ovens. Longer drying times are typically required, which leads to higher energy consumption and costs and lower production line speeds. Here, drying time is defined as the required time for a material to dry to the minimum moisture content at the given conditions. In order to optimize the process, drying by high-intensity thermal radiation rather

Received 26 December 1997; accepted 13 February 1998.
The authors gratefully acknowledge the support of the National Science Council of the Republic of China through grant NSC85-2212-E-009-006.
Address correspondence to Jenn-Der Lin, Department of Mechanical Engineering, National Chiao Tung University, 1001 Ta Hsueh Road, Hsinchu, Taiwan 30050, R.O.C.

Numerical Heat Transfer, Part A, 33:851–873, 1998

1040–7782/98 $12.00 + .00

NOMENCLATURE

d	location normalized to the thickness of the polymer solution ($= x/s$)	θ	dimensionless temperature ($= T/T_0$)
$\overline{D}$	dimensionless mass diffusion coefficient ($= D/\alpha_2$)	$\mathring{\rho}$	density
N	conduction to radiation parameter ($= k_2\beta_0/4\sigma T_0^3$)	ρ^d	diffuse reflectivity
Q_{in}, Q^r	dimensionless radiative energy input and flux, respectively ($= q_{in}/4\sigma T_0^4, q^r/4\sigma T_0^4$)	τ_{02}	optical thickness of substrate
		τ_1, τ_2	optical distance ($= \beta_{eff}x, \beta_0 x$)
		ϕ	intermittency
		ψ	dimensionless radiative intensity ($= \pi I/\sigma T_0^4$)
R	dimensionless drying rate	ω	mass fraction
s	geometric thickness		
S	dimensionless geometric thickness of solution layer ($= s/s_0$)	**Subscripts**	
W	percentage of residual weight compared to initial weight	A	water
		B	polymer
x	distance	c	convective stage
$y, \hat{y}$	dimensionless mass fractions of water [$= (\omega_A - \omega_{Ae})/(\omega_{A0} - \omega_{Ae})$, $(\hat{\omega} - \omega_{Ae})/(\omega_{A0} - \omega_{Ae})$]	eff	effective value
		r	radiative stage
α	thermal diffusivity ($= k/\rho c_p$)	s	surface
ε_2	emissivity at the substrate surface	0	initial value
ζ	dimensionless time ($= \alpha_2\beta_0^2 t$)	1	polymer solution
ζ_i	period	2	substrate

than by conventional hot air has been used in a number of areas. Because of the strong penetration capacity of infrared radiation, the temperature distribution in products would be more uniform in infrared drying compared to convective heat drying, and the quality of products could be improved. Stephansen [1] showed that the use of high-intensity, high-frequency infrared heaters improves printability of paper. The benefits of infrared radiation are also easy and rapid process control, clean environment, and straightforward heat transfer. Fundamental studies relating the applications of infrared radiation in drying have been the focus of attention in recent years.

In the last decades many studies were performed for analyzing heat and mass transfer in the convective heat drying process. Chen and Pei [2] presented an elaborate review for the transfer of heat and moisture in porous media by convective heating and also analyzed in detail the mass transfer mechanism during convective heating processes. In terms of the analysis of thermal radiation drying processes, few works were found. Nishimura et al. [3, 4] presented an investigation on the radiative heating and moisture redistribution process of aqueous polymer solution in which the temperature gradients inside a polymer solution and a substrate were neglected. Cote et al. [5] showed that the contribution to the variations of water content of convective air heating was small compared to that of radiation heating, but convective heat can remove the evaporated water vapor to increase the drying rate. The drying rate is defined as the amount of water content removed from the dried material in a unit of time per unit of drying surface, i.e., the rate of water content removal. Navarri and Andrieu [6] investigated moisture

redistribution processes of a thin wet sand layer under intensive infrared radiation. They showed that drying rates and solid temperature data were much higher than under conventional convective heating. However, they assumed that IR radiation was absorbed at the surface of the product. Chen and Lin [7] presented the radiative drying process of a polymer solution theoretically, and the results were analyzed in terms of a thermal field of solution layers. In their study, the influences of radiative properties of a polymer solution on drying were examined in detail. They also checked the validity of a lumped-system assumption in the thermal field during the heat and moisture transfer.

A drying process that includes both active stages and tempering stages is a drying process by intermittent heating. Drying by intermittent heating has been examined and a few studies were presented. In these studies, it was assumed that there was no external moisture transfer during the tempering stages. It is thus called intermittent drying. Brook and Bakker-Arkema [8] noted the possibility of obtaining higher quality dried corn from an intermittent drying process than from a continuous drying process. Toyoda [9] developed a two-tank model to predict the intermittent drying process of rough rice and showed that a high drying rate could be obtained after the tempering stages. Dostie et al. [10] studied the evolution of total mass during the intermittent radiative and continuous convective drying for an optically thick porous material. They assumed that there is no bulk water movement in the porous medium. The modeling of heating by infrared radiation had also been simplified, and the influence of radiation penetration was neglected. It was demonstrated that drying time can be reduced considerably by intermittent drying compared with convection drying alone, and drying by using intermittent infrared with convection drying improved drying efficiency and increased production rates. Zhang and Litchfield [11] indicated that an intermittent drying process with the tempering stage could reduce net heating time as well as energy consumption, compared with a continuous drying process. Franca et al. [12] showed that continuous drying was more efficient than intermittent drying in terms of drying time. However, intermittent drying could cause a significant improvement in grain quality. Chafe [13, 14] showed that intermittent drying could produce high-quality dried wood. Jumah et al. [15] showed that significant energy and quality advantages might accrue from intermittent drying of heat-sensitive particles. Chen and Lin [16] investigated the influences of various drying stages and external heating on the drying characteristics. Carroll and Churchill [17] numerically studied the intermittent heating process for homogeneous materials without phase change. They summarized that for the same amount of energy absorbed by the material, the increase of surface temperature is less for intermittent heating than for continuous heating.

The drying process for coatings is a complex problem involving the transfer of heat and mass in polymeric solutions. The objectives of the present study are to establish a mathematical model to completely simulate the heat and moisture transfer process of polymer solution by intermittent radiative heating in which the combined radiation and conduction heat transfer are involved, while in the substrate the mechanism of conduction heat transfer is utilized. We consider that the diffusion of liquid in the polymer solution follows Fick's law. The mass diffusion coefficient and equilibrium vapor pressure of water in the polymer solution are

assumed functions of mass fraction and temperature. We solve for the temperature and mass fraction distributions of the polymer solution during the drying process, and the effects of various radiation and convection parameters on heat and mass transports in solution are then examined. In addition to the energy consumption and flexible heating conditions, the drying process by intermittent heating is considered. In the present study, instead of the condition of no external moisture transfer during the tempering stage in the intermittent process that was considered by others, natural convective drying is included for this stage to simulate the real-life ambient air condition. We investigate the influences of various drying stages and external heating designs on the heat and mass transfer characteristics in the solution layer in terms of the drying rate, temperature, and moisture distributions.

MATHEMATICAL MODEL

A physical configuration under our investigation for the transfer of heat and mass of the solution layer that is exposed to high-intensity thermal radiation and/or an airflow is presented in Figure 1. The origin of the coordinate is fixed at the solution surface. We consider a polymer solution layer on a substrate of finite thickness, in which the lateral variations in composition and temperature are examined. The combined conduction and radiation heat transfer modes are considered in the polymer solution, while the substrate is assumed to be optically thick and thermal radiation interacting with the substrate is only a boundary phenomenon at the interface between the solution and the substrate. The convective contribution to heat transfer in the polymer solution is excluded. We include the airflow at specified temperature and relative humidity, which removes the water evaporated from the solution. As no forced airflow is supplied, natural convection would be the mechanism that brings the water vapor out of the solution surface. Furthermore, we assume local thermodynamic equilibrium within each macroscopically small averaging volume; that is, there is no temperature difference between the polymer and the water at any cross section in the polymer solution. During the drying processes, the main mechanisms of moisture transfer are assumed to be the diffusion of liquid through the polymer and evaporation of the liquid from the surface. The liquid is driven by the gradient of mass fraction. The diffusion obeys Fick's second law, but the mass diffusion coefficient shows strong concentration

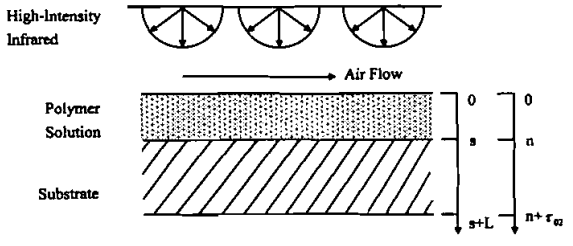

Figure 1. Physical configuration with geometric and optical coordinates.

and temperature dependence. As the intermittent heating process is studied, we consider it as two stages and refer to them as the radiative stage, during which radiative heating is applied, and as the convective stage, where no radiant heat input is supplied and only natural or forced convective heating is applied. Convective heating may exist in the radiative stage.

The governing equations for a one-dimensional transient energy and mass transfer problem can be written as follows in terms of nondimensional parameters to predict the unsteady temperature of polymer solution and substrate and mass fraction of water [16]. They are

$$\frac{\partial \theta_1}{\partial \zeta} + \frac{dS}{d\zeta}\frac{\partial \theta_1}{\partial \tau_1}\frac{[n(\zeta)-\tau]}{S} = \frac{\partial}{\partial \tau_1}\left[\left(\frac{\beta_{\text{eff}}}{\beta_0}\right)^2 \frac{\alpha_{\text{eff}}}{\alpha_2}\frac{\partial \theta_1}{\partial \tau_1}\right] - \left(\frac{\beta_{\text{eff}}}{\beta_0}\frac{\alpha_{\text{eff}}}{\alpha_2}\frac{k_2}{k_{\text{eff}}}\right)\frac{1}{N}\frac{\partial Q'}{\partial \tau_1} \qquad 0 < \tau_1 < n(\zeta) \quad (1)$$

$$\frac{\partial \theta_2}{\partial \zeta} = \frac{\partial^2 \theta_2}{\partial \tau_2^2} \qquad n(\zeta) < \tau_2 < n(\zeta) + \tau_{02} \quad (2)$$

$$\frac{\partial y}{\partial \zeta} + \frac{dS}{d\zeta}\frac{\partial y}{\partial \tau_1}\frac{[n(\zeta)-\tau_1]}{S} + \frac{2\bar{D}}{y+\hat{y}}\left(\frac{\beta_{\text{eff}}}{\beta_0}\frac{\partial y}{\partial \tau_1}\right)^2 = \frac{\partial}{\partial \tau_1}\left[\left(\frac{\beta_{\text{eff}}}{\beta_0}\right)^2 \bar{D}\frac{\partial y}{\partial \tau_1}\right] \qquad 0 < \tau_1 < n(\zeta) \quad (3)$$

where β_0 is the initial absorption coefficient and $dS/d\zeta$ represents the dimensionless drying rate, which can be then obtained as

$$R = -\frac{dS}{d\zeta} = -\frac{h_m(P_a - P)}{\alpha_2 \beta_0^2 s_0 \mathring{\rho}_A} \quad (4)$$

The second term on the left-hand side of Eqs. (1) and (3) exists due to the moving boundary. Here α_{eff} and k_{eff} are the effective thermal diffusivity and conductivity of the solution layer, respectively. These physical properties are dependent on the local liquid density and vary with the composition of solution. They are expressed in the following forms under the assumption that the volumetric additivity between the solvent and the solute is applicable to the solution:

$$\alpha_{\text{eff}} = k_{\text{eff}}/\left[c_{pA}(\rho_{A0} - \mathring{\rho}_A + \mathring{\rho}_A S) + c_{pB}(\rho_0 - \rho_{A0})\right] \quad (5)$$

$$k_{\text{eff}} = [k_A(\rho_{A0} - \mathring{\rho}_A + \mathring{\rho}_A S) + k_B(\rho_0 - \rho_{A0})]/(\rho_0 - \mathring{\rho}_A + \mathring{\rho}_A S) \quad (6)$$

where ρ_0 and ρ_{A0} are initial concentration of polymer solution and water and are given by

$$\rho = \frac{\mathring{\rho}_B \hat{\omega}}{\omega_A + \hat{\omega}} \tag{7}$$

$$\rho_A = \omega_A \rho \qquad \rho_B = (1 - \omega_A)\rho \tag{8}$$

with

$$\hat{\omega} = \frac{\mathring{\rho}_A}{(\mathring{\rho}_B - \mathring{\rho}_A)} \tag{9}$$

The solution medium is considered to be radiatively absorbing and emitting and gray. The variation of the optical thickness depends on the composition of the solution. The relation between geometric thickness s and optical thickness of the solution layer $n(\zeta)$ is given as

$$n(\zeta) = \left(s - \frac{\rho_{B0} s_0}{\mathring{\rho}_B}\right)\beta_A + \frac{\beta_{B0} s_0}{\mathring{\rho}_B}\beta_B \tag{10}$$

The effective absorption coefficient β_{eff} is expressed as

$$\beta_{eff} = \left(1 - \frac{\rho_{B0} s_0}{\mathring{\rho}_B s}\right)\beta_A + \frac{\rho_{B0} s_0}{\mathring{\rho}_B s}\beta_B \tag{11}$$

For the polymer solution the spectral absorption coefficient is greater than 10^4 m^{-1} in the wavelength range of 2.5–10 μm. Thus the mean absorption coefficient is also large even under the present gray assumption. Then the effect of radiation emission cannot be negligible even while the solution temperature is low. The radiation contribution in Eq. (1) can be expressed as

$$\frac{\partial Q^r}{\partial \tau_1} = (\theta_1^4 - G^*) \qquad 0 < \tau_1 < n(\zeta) \tag{12}$$

with nondimensional incident radiation G^* being obtained from the following transfer equation of radiation.

In the present model, we assume that water evaporation takes place only at the surface and that the bottom of the substrate is adiabatic. The initial and boundary conditions for the energy equations are thus as follows:

$$\theta_1 = \theta_2 = \theta_0 \qquad \zeta = 0 \tag{13}$$

$$-\frac{k_{eff}}{k_2}\frac{\beta_{eff}}{\beta_0}\frac{\partial \theta_1}{\partial \tau_1} = \frac{\mathring{\rho}_A}{\rho_2}\frac{n(0)}{\mathrm{Ja}}\frac{dS}{d\zeta} - \mathrm{Bi}(\theta_1 - \theta_\infty) \qquad \tau_1 = 0 \tag{14}$$

$$\frac{\beta_{eff}}{\beta_2}\frac{k_{eff}}{k_0}\frac{\partial \theta_1}{\partial \tau_1} = \frac{\partial \theta_2}{\partial \tau_2} + \frac{Q^r}{N} \qquad \theta_1 = \theta_2 \qquad \tau_1 = n(\zeta) \tag{15}$$

and

$$\frac{\partial \theta_2}{\partial \tau_2} = 0 \qquad \tau_2 = n(\zeta) + \tau_{02} \tag{16}$$

where Ja is the Jacob number, which is the ratio of sensible to latent energy absorbed during liquid-vapor phase change and Bi is the Biot number:

$$\mathrm{Ja} = \frac{c_{p2} T_r}{\gamma_A} \qquad \mathrm{Bi} = \frac{h}{k_2 \beta_0}$$

Here γ_A is the latent heat of water at the evaporation temperature and h is the convective heat transfer coefficient.

The transfer equation of radiation is expressed as

$$\mu \frac{\partial \psi(\tau_1, \mu)}{\partial \tau_1} + \psi(\tau_1, \mu) = \psi_b(\tau_1) \qquad 0 < \tau_1 < n(\zeta) \qquad -1 \leqslant \mu \leqslant 1 \tag{17}$$

The nondimensional incident radiation can be expressed in terms of the nondimensional radiation intensity $\psi(\tau_1, \mu)$ as

$$G^* = \frac{1}{2} \int_{-1}^{1} \psi(\tau_1, \mu)\, d\mu \qquad 0 < \tau_1 < n(\zeta) \tag{18}$$

Since the diffuse incidence of thermal radiation upon the semitransparent boundary of the solution layer is considered and at the interface between the substrate and polymer solution the substrate may emit, absorb, and reflect thermal radiation, the radiation boundary conditions are expressed as

$$\psi(0, \mu) = \frac{(1 - \rho_1'^{\mathrm{d}}) Q_{\mathrm{in}}}{\pi} f + 2\rho_1^{\mathrm{d}} \int_0^1 \psi(0, -\mu')\mu'\, d\mu' \qquad 0 \leqslant \mu \leqslant 1 \tag{19}$$

and

$$\psi[n(\zeta), -\mu] = \varepsilon_2 \theta_1 [n(\zeta)]^4 + 2\rho_2^{\mathrm{d}} \int_0^1 \psi[n(\zeta), \mu']\mu'\, d\mu' \qquad 0 \leqslant \mu \leqslant 1 \tag{20}$$

where $\rho_1'^{\mathrm{d}}$ and ρ_1^{d} are the external and internal reflectivities of the air-solution interface, respectively, ρ_2^{d} is the reflectivity of the solution-substrate interface, all calculated from Fresnel's equations, and f is the intermittence function that depends upon the control parameters used; $f = 1$ if $M \leqslant \zeta/\zeta_i \leqslant M + \phi$ and $f = 0$ if $M + \phi \leqslant \zeta/\zeta_i \leqslant M + 1$, where $M = 0, 1, 2, 3 \ldots$, is the number of complete cycles, ζ_i is the period for one cycle of radiative stage and convective stage, and ϕ is the intermittency (fraction of cycle during which radiative heat input is applied).

Under the assumption that the substrate is impermeable, the corresponding initial and boundary conditions for the mass transfer equation are

$$y = 1 \qquad \zeta = 0 \tag{21}$$

$$\bar{D}\frac{\partial y}{\partial \tau_1} = \frac{h_m(P - P_a)(y + \hat{y})}{\hat{\omega}^{2\circ}\hat{\rho}_A\,\mathring{\rho}_B\,\alpha_2\,\beta_{eff}} \times\left\{[(\omega_{A0} - \omega_{Ac})y + \omega_{Ac}]\left(\mathring{\rho}_A - \mathring{\rho}_B\hat{\omega}\right) + \mathring{\rho}_A\hat{\omega}\right\} \qquad \tau_1 = 0 \tag{22}$$

and

$$\frac{\partial y}{\partial \tau_1} = 0 \qquad \tau_1 = n(\zeta) \tag{23}$$

where h_m is the convective mass transfer coefficient. Both the dimensionless mass diffusion coefficient $\bar{D}$ and vapor pressure of water at the surface P are strongly dependent on temperature and moisture mass fraction in solution [18] and $\bar{D}$ increases with temperature following an Arrhenius law. They are given by

$$\bar{D} = \frac{1}{\alpha_2}\exp\left[\sum_{n=1}^{8}(1 - \omega_A)^{n-1}F_n + \frac{\Delta E}{R}\left(\frac{1}{298.15} - \frac{1}{T}\right)\right] \tag{24}$$

where F_n $(n = 1, 2, \ldots, 8)$ is -14.20662, 0.7050937, -92.66516, 718.8218, -2233.989, 3310.831, -2341.191, and 627.7167. ΔE $(= 7.3$ kcal/mol) is the Arrhenius activation energy, R is a gas constant, and

$$P = P_{s,T} \times a(\omega_A) \tag{25}$$

with $P_{s,T}$ being the saturated pressure of water vapor at temperature T (K) expressed as [19]

$$\log_{10}\frac{P_{cr}}{P_{s,T}} = \frac{\tilde{\theta}}{T}\frac{a_1 + a_2\tilde{\theta} + a_3\tilde{\theta}^3 + a_4\tilde{\theta}^4}{1 + a_5\tilde{\theta}} \tag{26}$$

where $P_{cr} = 22.11$ MPa, $\tilde{\theta} = T_{cr} - T$, $T_{cr} = 647.4$ K, $a_1 = 3.34613$, $a_2 = 4.14113 \times 10^{-2}$, $a_3 = 7.515484 \times 10^{-9}$, $a_4 = 6.56444 \times 10^{-11}$, $a_5 = 1.3794481 \times 10^{-2}$, and $a(\omega_A)$, which is the activity at the concentration of ω_A, given by

$$a = 1 \qquad \frac{\rho_B}{\mathring{\rho}_B} \leqslant 0.572 \tag{27}$$

$$a = \sum_{n=1}^{7}\left(\frac{\rho_B}{\mathring{\rho}_B}\right)^{(n-1)}F_n' \qquad \frac{\rho_B}{\mathring{\rho}_B} > 0.572 \tag{28}$$

F_n' ($n = 1, 2, \ldots, 7$) values in the expression are -6.000924, 33.63109, -51.77314, 31.54351, -36.5868, 64.65406, and -35.46261. Here the activity of water at the surface becomes a function of the water mass fraction, while $\rho_B/\mathring{\rho}_B > 0.572$, which corresponds to the water mass fraction of 0.3685 at the surface. P_a is partial pressure of water vapor in air. It can be represented as

$$P_a = \frac{\omega_H P_\infty}{(\omega_H + 0.622)} \tag{29}$$

where ω_H is the humidity ratio and P_∞ is atmospheric pressure.

NUMERICAL METHODOLOGY

The numerical technique employed to solve the set of nonlinear energy and mass transfer equations is the fully implicit time discretization scheme, which is used to allow for larger time steps. Linearization is accomplished by evaluating the nonlinear coefficients at the previous time step. The central difference for the spatial derivatives in these equations is used. To deal with the moving boundary problem, we use the time-dependent coordinate systems [20], i.e., the variable grid space at fixed grid number is utilized to numerically solve the system of partial differential equations. The time derivative term in the transformed plane can be shown as

$$\left.\frac{\partial u}{\partial t}\right|_{\text{physical}} = \left.\frac{\partial u}{\partial t}\right|_{\text{transformed}} + \frac{dx}{dt}\frac{\partial u}{\partial x} \tag{30}$$

Note that in the transformed expression for the time derivatives, all derivatives are taken at the fixed grid points in the transformed plane. The movement of the grid in the physical plane is reflected only through the rates of change of x at the fixed grid points in the transformed plane.

The radiation contribution is solved by the P3 approximation technique [21], since it is difficult to obtain the exact solution of the radiation distribution. The nondimensional intensity of radiation is represented as

$$\psi(\tau_1, \mu) = \sum_{m=0}^{3} \frac{2m+1}{4} P_m(\mu)\varphi_m(\tau_1) \tag{31}$$

Substitution of Eq. (31) into the radiative transfer equation, Eq. (17), results in four sets of ordinary differential equations for the functions $\varphi_m(\tau_1)$. To solve the four equations, we utilize Marshak's boundary conditions to approximate the radiative boundary conditions for the P3 scheme. The subroutine DBVPFD of the IMSL package in HP 9000/735 is used to solve the above associated first-order ordinary differential equations. By applying the orthogonality of the Legendre polynomials $P_m(\mu)$, we obtain that $G^*(\tau_1) = \varphi_0(\tau_1)/4\pi$ and $Q^r(\tau_1) = \varphi_1(\tau_1)/4\pi$. In numerical computation, the radiation intensity is first solved and then substituted into the energy equation and boundary conditions to solve for the temperature distributions and, subsequently, to solve the mass transfer equation for mass fractions.

Since the nonlinear energy and mass transfer equations with moving boundary effect are solved, the alternating underrelaxation factor for temperature and mass fraction is employed in the iterative procedure to quicken the convergence of the solutions. At each time increment, the nodal values of temperature and mass fraction are solved iteratively, and convergence is checked on both variables. The parameters such as density of polymer solution, drying rate, thickness of solution, and radiative heat flux, which appear in the coefficients of finite difference equations, are initially evaluated with the use of these values obtained at the previous time step. Combined with the boundary conditions, the Gauss elimination method is employed to solve for the variables at a new time level. If the convergent solution is not attained, the newly calculated variables are used to update the parameters for the next iteration. The procedure continues until convergence is found according to a prescribed condition (the maximum relative errors of both mass fraction and temperature are $< 10^{-3}$ in the present study). This procedure is carried out repeatedly along the time axis. The grid systems have 401 grid points in the polymer solution and in the substrate, and these grids have been checked to ensure grid-independent results.

In addition, the self-consistency of the polymer solution is also checked by a total mass balance:

$$W_{1,0} = s_0 \rho_0 \tag{32}$$

$$W_{1,t} = \int_0^t -\mathring{\rho}_A \frac{dS}{dt'} dt' + \mathring{\rho}_B \hat{\omega} \int_0^s \frac{1}{\omega_A + \hat{\omega}} dz \tag{33}$$

where $W_{1,0}$ and $W_{1,t}$ are the mass of polymer solution at time 0 and t, respectively. In Eq. (33), the first term refers to the water evaporated from the very beginning to time t, and the second term refers to the mass retained in the polymer solution. During the calculations, the mass evaluated through Eq. (33) varied by no more than 1.0%, that is,

$$\left| \frac{W_{1,t} - W_{1,0}}{W_{1,0}} \right| < 0.01 \tag{34}$$

Then we define the mass percentage of residual polymer solution and water as

$$W = \mathring{\rho}_B \hat{\omega} \int_0^s \frac{1}{\omega_A + \hat{\omega}} dz \Big/ W_{1,0} \tag{35}$$

and

$$W_A = \mathring{\rho}_B \hat{\omega} \int_0^s \frac{\omega_A}{\omega_A + \hat{\omega}} dz \Big/ W_{A,0} \tag{36}$$

where $W_{A,0}$, the mass of water at time 0, can be expressed as

$$W_{A,0} = \frac{\omega_{A0} \mathring{\rho}_B}{\omega_{A0} \mathring{\rho}_B + (1 - \omega_{A0}) \mathring{\rho}_A} s_0 \mathring{\rho}_A \tag{37}$$

RESULTS AND DISCUSSION

In the following we show the transfer of heat and moisture in polymer solutions on a substrate exposed to radiative heating at various convection and radiation parameters. The nondimensional initial temperatures of polymer solution and substrate are 1.0, i.e., at the temperature of the environment. From Fresnel's equations, the internal and external reflectivities of the air-solution interface and the reflectivity of the substrate are found. The $\rho_1'^{\mathrm{d}}$ is taken as 0.094 and ρ_1^{d} as 0.448 by averaging the directional reflectivity, and they are less dependent on wavelength in our computations. Aluminum and glass plates are used as the substrates in our results. The complex indices of refraction of the substrate can be used to calculate the reflectivity of the interface between the polymer solution and the substrate [21], and ρ_2^{d} for the aluminum plate is taken as 0.903 and for the glass plate as 0.089. The composition of solution varies during moisture transfer, and consequently, the complex refractive index of solution varies. The physical properties for different compositions are weighted in proportion to the composition. The real part of the refractive index of solution is between 1.33 and 1.5 in our calculations, since that of water is 1.33 and polyvinylalcohol (PVA) is 1.5. The imaginary part of the refractive index can be obtained from the radiative absorption coefficient [22]. The absorption coefficient of water and PVA ranges from 1 to 10^5 for the radiation wavelength of 0.7–10.0 μm [3], from which we get the imaginary part of the refractive index of solution that is between 0.005 and 0.2. Thermal conductivities of the substrate of aluminum, glass plate, water, and PVA used here are 204, 0.78, 0.604, and 0.169 W m^{-1} K^{-1} [23], respectively. In numerical calculations, the heat transfer coefficient h of 30 W m^{-2} K^{-1}, which corresponds to application of an airflow with a parallel speed of 2.5 m s^{-1}, and convective mass transfer coefficient h_m of 1.7×10^{-7} kg m^{-2} s^{-1} Pa^{-1} [18] are used. While no forced convection airflow applies, natural convection is included and $h = 6.5$ W m^{-2} K^{-1} [23] and h_m obtained by an analogic relation (i.e., 3.81×10^{-8} kg m^{-2} s^{-1} Pa^{-1}) are utilized [24]. The humidity ratio of ambient air ω_{H} is taken as 0.0047. The initial thickness of the solution layer s_0 is 2.5×10^{-3} m with initial water mass fraction $\omega_{\mathrm{A0}} = 0.95$ by weight. In the following, we make a comparison of the transfer of heat and moisture in polymer solution layers with intermittent and continuous heating by radiation and convection, and also examine the influences of the various convection and radiation parameters on heat and mass transfer processes. Radiative heating is applied during the radiative stage, and the radiative stage is applied first in a cycle. The duration of the radiative stage is $\zeta_i \phi$ and that of the convective stage is $\zeta_i(1 - \phi)$. The parameters of the above values are used unless noted otherwise.

The influences of intermittency ϕ on transient moisture and heat transfer processes at $Q_{\mathrm{in}} = 1.0$, $n(0) = 25$, $\zeta_i = 40{,}000$, and $\mathrm{Bi}_{\mathrm{r}} = 1.0 \times 10^{-3}$ are plotted in Figures 2 and 3. Bi_{r} represents the Biot number associated with the air condition during the radiative stage. Bi_{c}, equal to 3.25×10^{-4}, is utilized during the convective stage, which corresponds to the case of heat transfer by natural convection. Figure 2 shows the variations of the percentage of residual weight compared to initial weight of polymer solution W, surface temperature of polymer solution θ_{s}, and drying rate R with respect to time. The predicted water mass

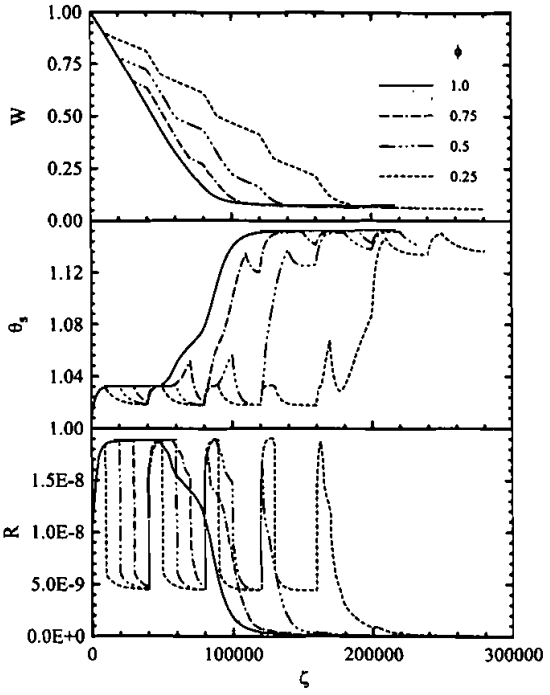

Figure 2. Variations of solution weight, surface temperature, and drying rate with respect to time at various intermittency.

fraction distributions at various times within the polymer solution are also presented in Figure 3. Because of the evaporation of water, the boundary is moving and the thickness of the polymer solution is changing. The d in the figure represents the location normalized to the thickness of the solution layer, and the solution surface is located at $d = 0$. In regard to the drying mechanism in the continuous heating process ($\phi = 1$), it is seen that while the external mass transfer for water vapor and radiative heat input are applied, the drying rate increases initially. Temperatures of solution also increase, since not much latent heat is required and part of the energy input is to increase the sensible heat. After this early drying process, θ_s reaches an equilibrium temperature because the moisture of the product is abundant near the surface and the energy input is balanced by the evaporation of water. It is also found that moisture removal proceeds at a nearly constant rate because the partial pressure difference of water vapor between the surface and the ambient air is almost constant. The water mass fraction at the surface decreases but is still higher. The variation of the water content is independent of the distribution of the water mass fraction in the polymer solution and is controlled by the convection and radiation parameters. This is the so-called constant rate period. The diffusion coefficient in the solution is larger at higher temperatures and higher water concentration. The higher the mass diffusion coefficient is in the interior region of the polymer solution, the more water can

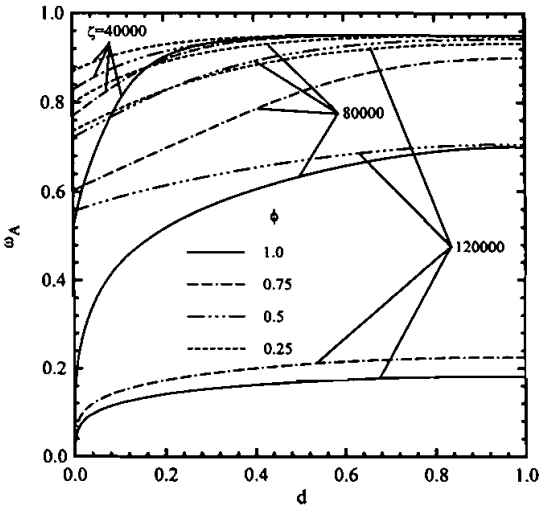

Figure 3. Water content distributions at various times for various intermittency.

diffuse from the interior region to the surface. The activity is dependent on the surface water mass fraction. Since the activity is large, the vapor pressure difference between the solution surface and the ambient air is large, and the rate of water content removal is large. After the constant rate period, the surface water mass fraction continues to drop, since water density near the internal region is transported to the surface at a lower rate than that at which evaporation occurs. This leads to a slower drying rate due to the effect of activity. The rate of water content removal is dominated by the water mass fraction profile in the polymer solution. Thus the drying rate decreases and the temperature increases rapidly. Because of the higher temperatures in polymer solutions, the solution emits larger radiative energy to the ambient air and lower radiative energy can be absorbed in the polymer solution and substrate. This is the so-called falling rate period. While considering the intermittent heating process ($\phi < 1$), the radiative stage ensues initially. It is noticed that the heat and moisture transfers in this stage are the same as those in the continuous heating process. During the natural convective stage, the convective mass transfer coefficient is small, and there is lack of radiative energy input. The drying rate drops to a very small value, and surface temperature also drops. The water near the bottom of the polymer solution diffuses toward the surface and then recovers near the upper region, since the mass transfer coefficient is less. Figure 3 illustrates that the water mass fraction near the solution surface is larger than that for the continuous heating process after the end of the convective stage. This phenomenon is similar to the tempering effect [9], as there is no external moisture transfer. It is also found that the slope of the water mass fraction profile near the surface is flatter for smaller ϕ, since there is more time for water to diffuse from the bottom to the surface and then to recover near the surface. In spite of the low drying rate during the natural convective stage, the effect of water

recovery near the surface enhances the drying rate during the radiative stage. While the radiative stage follows, the drying rate in the case of intermittent heating is larger than that of continuous heating as shown in Figure 2. Because of the recovery of water near the solution surface during the natural convective stage, the drying rate increases rapidly with high-energy input and high water mass fraction near the surface as the radiative heating is imposed at the beginning of the following radiative stages. For $\phi = 0.75$ the drying rate increases rapidly as the radiation flux is incident, but the water diffused from the interior region cannot reach the surface immediately, and therefore the drying rate drops abruptly. For $\phi = 0.25$, more water mass fraction exists near the surface, and a higher drying rate can be obtained compared with the cases of higher ϕ. It is then found that the rate of water content removal is nearly equal to the drying rate in a constant rate period for short times, and surface temperature also stays at a constant value. It is also found that the drying rate remains large during the radiative stage of the next cycles. Although the drying rate can be improved more during radiative stages, more drying time is also required for smaller ϕ. Thus the drying process is completed almost at the same time for larger ϕ, which illustrates the savings of energy and time achieved.

The variations of water content with respect to time under the influence of ζ_i are plotted in Figure 4 at $Q_{in} = 1.0$, $n(0) = 25$, $\phi = 0.5$, $Bi_r = 1.0 \times 10^{-3}$, and $Bi_c = 3.25 \times 10^{-4}$. As ζ_i is small, the duration of the radiative stage is small. The decrease of water content near the upper region is slight during the radiative stage, and water near the surface can be supplied from the interior during the convective stage, which occurs soon thereafter. Though the amount of water evaporation is less during the early drying process, the amount of water evaporation is more for smaller ζ_i after a few cycles of intermittent heating. Drying processes with more

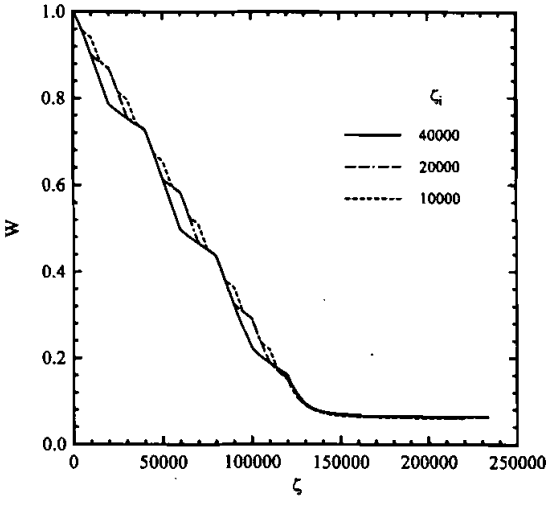

Figure 4. Variations of solution weight with respect to time at various periods of one cycle.

cycles are better when the drying time is the main concern, but the discrepancy in the variations of water content with time among these cases is not manifest.

Figure 5 shows the transient behavior of the heat and mass transfer processes in polymer solution for different Bi_r at $Q_{in} = 1.0$, $n(0) = 25$, $\zeta_i = 40{,}000$, $Bi_c = 3.25 \times 10^{-4}$, and $\phi = 0.5$ and 1.0. For $\phi = 0.5$ the drying rate increases to a higher value, since the heat and mass transfer coefficients are larger at higher Bi_r. More water near the surface is evaporated, the duration of the constant drying rate period is smaller, and the temperatures of solution are lower. After the constant rate period, the drying rate decreases, and the solution temperature increases, and more latent heat is required because of the higher surface temperature. So the drying rate for cases of higher Bi_r drops to a smaller value. During the first radiative stage, the constant rate period has not yet ended for $Bi_r = 1 \times 10^{-3}$. After water moisture is redistributed during the convective stage, we find that the constant rate period appears again during the second radiative stage. This causes more water evaporation. In contrast to the phenomena during the first radiative stage, the usage of smaller external transfer conditions improves the drying rate during the second radiative stage. When the third radiative stage begins, the drying rate is the largest for $Bi_r = 1 \times 10^{-3}$, since the surface water mass fraction is abundant. The diffusion in the polymer solution is greater for higher temperature distribution, and the drying rate stays higher for smaller Bi_r. Thus it is illustrated that a higher convective transfer coefficient cannot definitely reduce the required drying time. Similar results for the continuous heating process, i.e., $\phi = 1.0$, are also shown in Figure 5. The amount of water evaporated becomes less for larger Bi_r after a period of drying time. This time period is shorter for continuous heating compared to the results for intermittent heating processes. Because the water

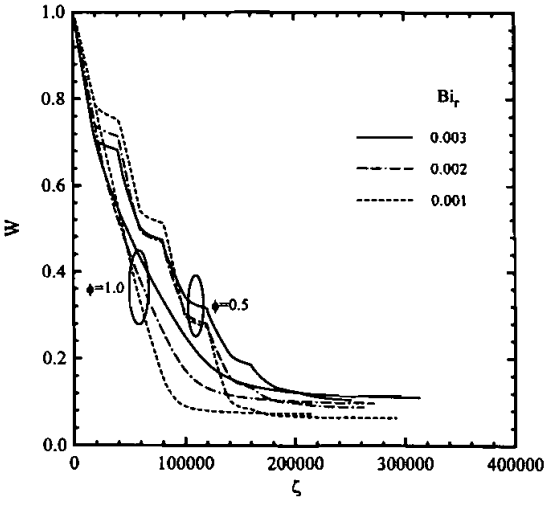

Figure 5. Variations of solution weight with respect to time at various Biot numbers during the radiative stage.

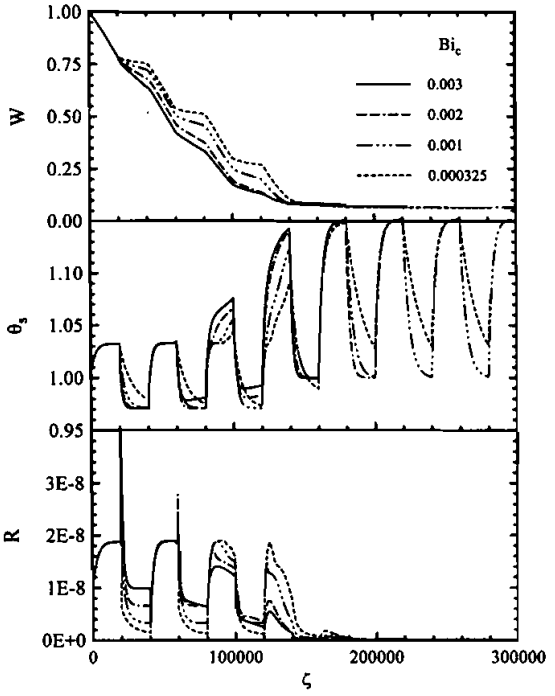

Figure 6. Variations of solution weight, surface temperature, and drying rate with respect to time at various Biot numbers during the convective stage.

content near the surface can be supplied much more during the convective stage at $\phi = 0.5$, the drying rate can be enhanced during the radiative stage. Figure 6 presents variations of W, θ_s, and R with respect to time for various Bi_c at $Q_{in} = 1.0$, $n(0) = 25$, $\zeta_i = 40{,}000$, $Bi_r = 1.0 \times 10^{-3}$, and $\phi = 0.5$. The predicted distributions of ω_A at various times within the polymer solution are also presented in Figure 7. During the first convective stage, the drying rate with higher Bi_c is larger, since the higher external mass transfer is applied. However, the surface water mass fraction is smaller compared with the case of lower Bi_c after the convective stage is over. While the radiative stage continues, the drying rate after the natural convective stage is larger than that after the forced convective stage because of the recovery of water near the solution surface. It is shown that the slope of the W curves in Figure 6 during the radiative stage becomes smaller with higher Bi_c. During the following convective stages, similar results show that the rate of water content removal is gradually decreased for the case of higher Bi_c. Then the time required to complete the drying process is almost the same for all cases, and energy savings can be achieved if the natural convective stage is considered.

Figure 8 shows similar results for cases of various radiative energy input and various radiative stage periods during drying at $n(0) = 25$ and $Bi_r = 1.0 \times 10^{-3}$. Natural convective drying is applied during the convective stage, and total radiative

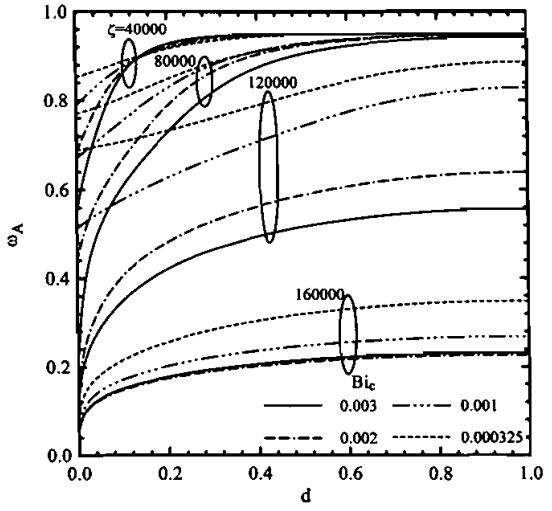

Figure 7. Water content distributions at various times for various Biot numbers during the convective stage.

energy input during the radiative stage is constant, that is, $Q_{in} \times \zeta_i \phi = 15{,}000$. Based on the same total amount of radiative energy input, variations in the percentages of water loss are shown in Figure 9 for several cases at the end of the first six radiative stages. Based on the same total amount of radiative energy input for the cases of $\zeta_i = 40{,}000$, the duration of the convective stage is larger as the input radiation energy Q_{in} is smaller. The water near the bottom of the polymer

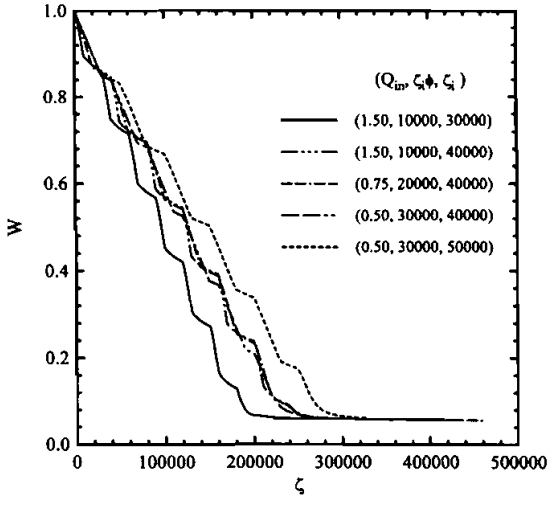

Figure 8. Variations of solution weight with respect to time at constant total radiative energy input.

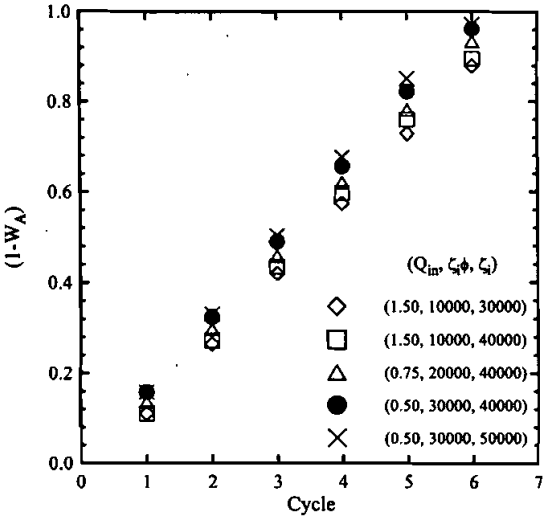

Figure 9. Percentages of water evaporated at the end of the first six radiative stages at constant total radiative energy input.

solution diffuses toward the surface and then recovers near the upper region, since the mass transfer coefficient is smaller during the convective stage. It is found in Figure 8 that the slope of the curves during the radiative stages is larger, i.e., the drying rate is larger, at fixed ζ_i than that of the cases with fixed duration of the convective stage. Although the duration of the convective stage is larger for larger Q_{in}, the required drying times for all cases are almost the same. As $\zeta_i(1 - \phi) = 20{,}000$, the duration of the convective stage is fixed. Although the rate of water content removal is larger for higher input of radiant heat, the temperatures of the polymer solution also increase sooner. Required energy for water evaporation increases, while the surface temperature of the polymer solution grows higher, so the required latent heat per unit mass of water is much greater. Therefore the variation of water content for the case of $Q_{in} = 1.5$ under equal total radiative energy input at the end of the radiative stage would be the lowest, as shown in Figure 9. As the water recovers near the surface during the convective stage and the following radiative stage begins, peaks in the drying rate profile are also found. The drying rate increases abruptly, and drops, and then increases again. For $Q_{in} = 1.5$, it is even noticed that the drying rate grows to a higher value than that of the peak. This occurs because the temperature of the polymer solution is high and the mass diffusivity is also high, so much of the internal water can diffuse quickly to the surface. It is also shown in Figure 9 that the percentages of residual-water weight are less for smaller Q_{in} than for larger Q_{in}. However, the large radiant energy input is mainly utilized as drying time, since the drying rate is dominated by the absorbed radiative energy.

Figure 10 presents the results for various values of absorption coefficient β at $Q_{in} = 1.0$, $\zeta_i = 40{,}000$, $Bi_r = 1.0 \times 10^{-3}$, $Bi_c = 3.25 \times 10^{-4}$, and $\phi = 0.5$. The

radiative absorption coefficients of PVA and water are $O(1)$ for the wavelength below 1 μm and $O(10^4)$ for wavelengths above 2.5 μm [3]. Here, three different values of absorption coefficients are used in our cases, which correspond to different sources of infrared heating. The radiation flux reaching the interface between the solution and the substrate will be absorbed and/or reflected. As the optical thickness is huge for the case of a large absorption coefficient at the beginning of the drying period, the absorption of radiant energy is thus nearly a surface phenomenon. For the case of small β, the effect of radiation reflection and absorption at the interface becomes significant. As an illustration, we consider aluminum plate as the substrate for which ρ_2^d is large; the radiation penetrating is reflected at the interface. The internal reflectivity of the air-solution interface is not huge; most radiation heat emitted and/or reflected from the substrate could not be reflected back toward the medium at the solution surface to reheat the polymer solution. Thus the absorbed radiative energy is smaller, and the drying rate is considerably decreased. The predicted results for intermittent heating at various β are shown in Figure 11 for the same conditions, but we consider the glass plate as the substrate, for which ρ_2^d is small. Most of the radiation flux reaching the interface will be absorbed by the substrate for smaller ρ_2^d. For the case of small β, less radiant energy could be absorbed in the polymer solution. However, the substrate absorbs the most radiant energy and then behaves as a heat source to heat the bottom of the polymer solution. Thus it is illustrated that the drying rate is dominated by the net amount of absorbed radiant energy, and the difference in drying rates among these cases is not distinct.

Figures 12 and 13 show the typical effects of initial temperatures of polymer solutions on the heat and mass transfer processes for $Q_{in} = 1.0$, $n(0) = 25$, $\phi = 0.5$, $Bi_r = 1.0 \times 10^{-3}$, and $Bi_c = 3.25 \times 10^{-4}$. Here the effect of preheating

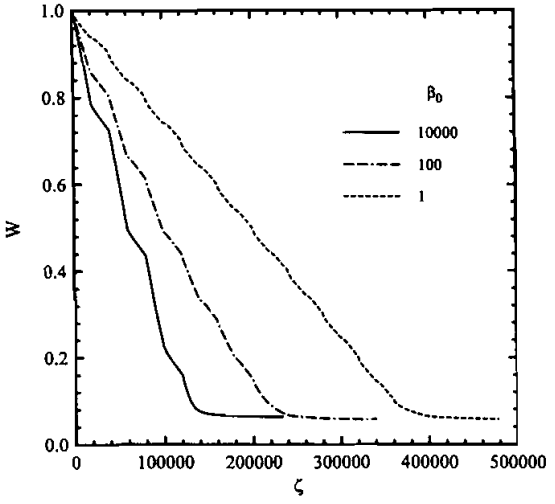

Figure 10. Variations of solution weight with respect to time at various absorption coefficients with small substrate reflectivity.

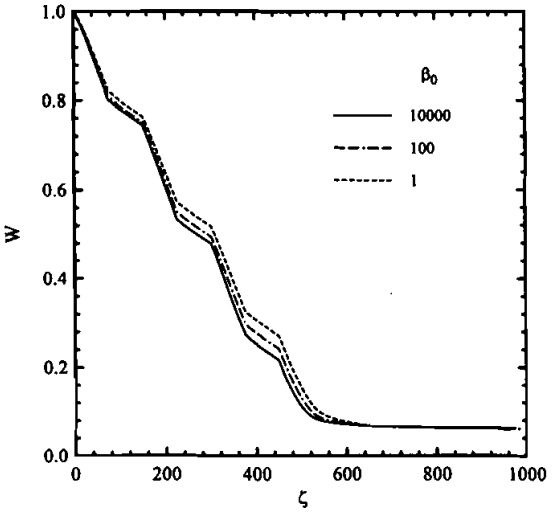

Figure 11. Variations of solution weight with respect to time at various absorption coefficients with large substrate reflectivity.

on drying processes is considered. As θ_0 is larger, the drying rate is larger due to a higher water vapor difference between the solution surface and the ambient air condition. Because there is not enough energy input from outside to support the higher latent heat required, the drying rate and temperature decrease and then reach constant values. In contrast to higher θ_0, the opposite results are shown during the early drying process for smaller θ_0. The initial temperatures of the polymer solution only affect the transfer of heat and moisture during the preliminary period, and then the drying rate and temperatures reach equilibrium values, since the drying rate is controlled by external heating conditions. The results are almost the same after the constant rate period begins. After the second cycle is over, the surface water mass fraction is still higher for all cases, but the residual water for the case of low θ_0 is larger, and the drying rate becomes larger as radiative heating is imposed again. The drying processes are completed at almost the same time for all cases. Thus the preheating effect of polymer solutions does not help in the reduction of drying time during the heat and moisture transfer processes.

CONCLUSION

The heat and mass transfer processes of polymer solutions that are intermittently exposed to high-intensity infrared radiation and/or airflow are theoretically investigated. We examine the effects of various radiation and convection parameters on the heat and mass transfer processes. Results show that a net amount of radiant energy absorbed by the solution layer and substrate has significant effects on the thermal field. The rate of water content removal is dominated not only by

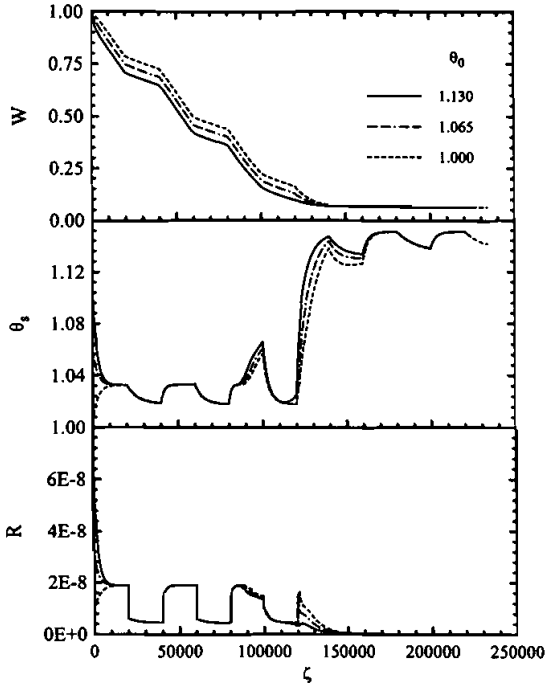

Figure 12. Variations of solution weight, surface temperature, and drying rate with respect to time at various initial temperatures.

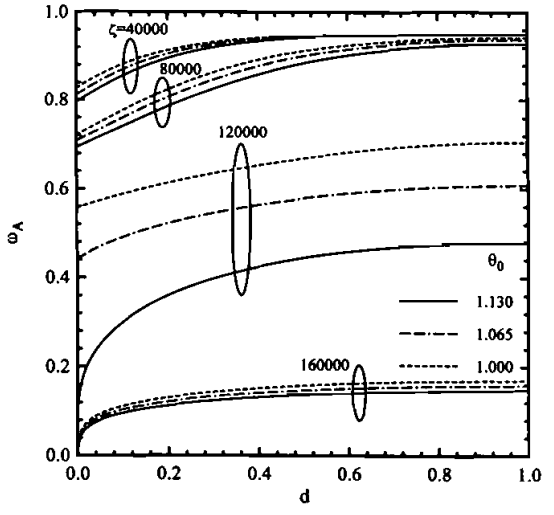

Figure 13. Water content distributions at various times for various initial temperatures.

the absorbed radiative energy, but also by the moisture distributions in the polymer solution. It is seen that the drying rate is higher with higher radiant energy absorbed and larger moisture mass fraction near the surface. Intermittent radiation heating can improve the temporary drying rate during the radiative stage because of the recovery of water near the surface of the polymer solution during the convective stage with small convective transfer parameters. While the energy efficiency and external heating design for industrial applications are concerned, drying processes with intermittent heating at larger intermittency are recommended for energy and time savings. Based on the same duration of the convective stage, a small amount of radiant energy is applied during the radiative stage in order to use energy efficiently, but a large radiation input is utilized when drying time is the major concern. However, the use of higher external transfer parameters during drying and the preheating of polymer layers before drying cannot reduce drying times.

REFERENCES

1. E. W. Stephansen, New High-Intensity Infrared Radiation Reduces Binder Migration on Coating, *TAPPI J.*, vol. 69, pp. 42–44, 1986.
2. P. Chen and D. C. T. Pei, A Mathematical Model of Drying Processes, *Int. J. Heat Mass Transfer*, vol. 32, pp. 297–310, 1989.
3. M. Nishimura, M. Kuraishi, and Y. Bando, Effect of Internal Heating on Infrared Drying of Coated Films, *Kagaku Kogaku Ronbunshu*, vol. 9, pp. 148–153, 1983.
4. M. Nishimura, M. Kuraishi, Y. Bando, and H. Kojima, Influence of the Spectral Distribution of Incident Radiation on the Effect of Internal Heating in Infrared Drying of Coated Films, *Kagaku Kogaku Ronbunshu*, vol. 10, pp. 124–126, 1984.
5. B. Cote, A. D. Broadbent, and N. Therien, Modeling and Simulating of Continuous Drying of Thin Layers by Infrared Radiation, *Can. J. Chem. Eng.*, vol. 68, pp. 786–794, 1990.
6. P. Navarri and J. Andrieu, High-Intensity Infrared Drying Study, Part I—Case of Capillary-Porous Material, *Chem. Eng. Proc.*, vol. 32, pp. 311–318, 1993.
7. J. J. Chen and J. D. Lin, Analysis of Heat and Mass Transfer in Drying Processes of Polymer Solution Using High-Intensity Infrared Radiation, in A. S. Mujumdar (ed.), *Drying '96*, pp. 93–102, Lodz Technical University, Poland, 1996.
8. R. C. Brook and F. W. Bakker-Arkema, Simulation for Design of Commercial Concurrent-Flow Grain Dryers, *Trans. ASAE*, vol. 21, pp. 978–981, 1978.
9. K. Toyoda, Study on Intermittent Drying of Rough Rice in a Recirculation Dryer, in A. S. Mujumdar and M. Roques (eds.), *Drying '89*, pp. 289–296, Hemisphere, New York, 1989.
10. M. Dostie, J. N. Seguin, D. Maure, Q. A. T. That, and R. Chatigny, Preliminary Measurements on the Drying of Thick Porous Materials by Combination of Intermittent Infrared and Continuous Convection Heating, in A. S. Mujumdar and M. Roques (eds.), *Drying '89*, pp. 513–519, Hemisphere, New York, 1989.
11. Q. Zhang and J. B. Litchfield, An Optimization of Intermittent Corn Drying in a Laboratory Scale Thin Layer Dryer, *Drying Technol.*, vol. 9, pp. 383–395, 1991.
12. A. S. Franca, M. Fortes, and K. Haghighi, Numerical Simulation of Intermittent and Continuous Deep-Bed Drying of Biological Materials, *Drying Technol.*, vol. 12, pp. 1537–1560, 1994.

13. S. C. Chafe, Preheating and Continuous and Intermittent Drying in Boards of *Eucalyptus regnans* F. Muell, I—Effect on Internal Checking, Shrinkage, and Collapse, *Holzforschung*, vol. 49, pp. 227–233, 1995.
14. S. C. Chafe, Preheating and Continuous and Intermittent Drying in Boards of *Eucalyptus regnans* F. Muell, II—Changes in Shrinkage and Moisture Content During Drying, *Holzforschung*, vol. 49, pp. 234–238, 1995.
15. R. Y. Jumah, A. S. Mujumdar, and G. S. V. Raghavan, A Mathematical Model for Constant and Intermittent Batch Drying of Grains in a Novel Rotating Jet Spouted Bed, *Drying Technol.*, vol. 14, pp. 765–802, 1996.
16. J. J. Chen and J. D. Lin, Theoretical Analysis on Drying of Polymer Solution with Continuous or Intermittent Heating by High-Intensity Infrared Radiation, presented at the Second International Symposium on Radiative Transfer, Kusadasi, Turkey, July 1997.
17. M. B. Carroll and S. W. Churchill, A Numerical Study of Periodic on-off Versus Continuous Heating by Conduction, *Numer. Heat Transfer*, vol. 10, pp. 297–310, 1986.
18. M. Okazaki, K. Shioda, K. Masuda, and R. Toei, Drying Mechanism of Coated Film of Polymer Solution, *J. Chem. Eng. Jpn.*, vol. 7, pp. 99–105, 1974.
19. S. Haber, A. Shavit, and J. Dayan, The Effect of Heat Convection on Drying of Porous Semi-Infinite Space, *Int. J. Heat Mass Transfer*, vol. 27, pp. 2347–2353, 1984.
20. J. F. Thompson, F. C. Thames, and C. W. Mastin, Automatic Numerical Generation of Body-Fitted Curvilinear Coordinate System for Field Containing Any Number of Arbitrary Two-Dimensional Bodies, *J. Comput. Phys.*, vol. 15, pp. 299–319, 1974.
21. M. N. Ozisik, *Radiative Transfer*, pp. 334–343, Wiley, New York, 1993.
22. M. F. Modest, *Radiative Heat Transfer*, 444 pp., McGraw-Hill, New York, 1993.
23. J. P. Holman, *Heat Transfer*, SI metric ed., 13 pp., McGraw-Hill, New York, 1989.
24. I. Savoye, G. Trystram, A. Duquenoy, P. Brunet, and F. Marchin, Heat and Mass Transfer Dynamic Modeling of an Indirect Biscuit Baking Tunnel-Oven, Part I—Modeling Principles, *J. Food Eng.*, vol. 16, pp. 173–196, 1992.